

Monitoring geological carbon storage: detection threshold at the CaMI Newell County Facility and a look ahead at a sparse monitoring approach for gigatonne scale storage

Don Lawton^{1,2}, Brendan Kolkman-Quinn^{1,2}, Marie Macquet² and Kris Innanen¹.

¹University of Calgary; ²Carbon Management Canada

ABSTRACT

Monitoring CO₂ injection at the CaMI Newell County Facility has continued with a broad range of monitoring technologies being implemented and evaluated. At the site, small volumes of CO₂ are being injected into a sandstone reservoir at 300 m depth, simulating a CO₂ leak from a deep geological carbon storage project. Time-lapse multi-offset and multi-azimuth vertical seismic profiles (VSP) and time-lapse electrical resistivity (ERT) surveys have both been successful at imaging less than 50 tonnes of CO₂ at this injection program. Detailed interpretation of the time-lapse data is that CO₂ has migrated up-section in the storage complex between 2021 and 2022. ERT time-lapse results also support this interpretation.

For seismic monitoring of large-scale geologic carbon storage projects there are 4 main challenges - repeatability, resolution, how often we repeat the seismic surveys, and the cost of full-scale surveys that extend over the anticipated area of the CO₂ plume and/or pressure front. One monitoring approach that we are proposing is to use sparse nodes of sub-permanent seismic sources and permanent receivers along with other monitoring technologies that can be deployed on an expanding basis during the injection program as the plume develops. The separation of the source and receivers will be determined by an optimum offset to maximize the signal-to-noise ratio of the reflections from the CO₂ storage zone.

INTRODUCTION

Geological carbon storage (GCS) is gaining rapid acceptance as a key technology to help meet greenhouse gas emissions reduction targets by 2030 and a net-zero carbon economy by 2050. The Newell County research facility has been developed jointly by Carbon Management Canada (CMC) and the University of Calgary to advance monitoring technologies for GCS. The facility is located 200 km south-east of Calgary in Newell County and full details are available from Lawton et al. (2019), Macquet et al. (2019) and Macquet et al., (2022). At this site we are injecting a small mass of CO₂ (several tens of tonnes/year) into the Basal Belly River Sandstone (BBRS) Formation at 300 m depth to simulate CO₂ leakage from a deeper, large-scale CO₂ storage project. The injection program is being monitored by a broad range of geophysical and geochemical technologies. The small, controlled amount of injected CO₂ has enabled us to determine the detection threshold for gas-phase CO₂ at shallow to intermediate depths, and to improve and develop monitoring technologies to verify secure geological carbon storage (GCS). In this report we review some of the time-lapse vertical seismic profile (VSP) and electrical resistivity tomography (ERT) data that has acquired, processed and interpreted collaboratively

between CMC and CREWES and we also look ahead at a new approach to monitoring large scale GCS projects.

MONITORING RESULTS

Time-lapse VSP data

Time-lapse monitoring with Vertical Seismic Profiles (VSP) in Observation Well #2 (Obs2) began in 2017 and successfully imaged the CO₂ plume by March, 2021, after 32 tonnes of cumulative CO₂ injection (Kolkman-Quinn et al., 2022a,b). Obs2 is located 20 m SW of the CO₂ injection well. Figure 1 shows the difference between baseline and monitor VSP CDP sections from surveys spanning 2017-2022. By 2019, the seismic signature of the 14 t CO₂ plume remained ambiguous amid background amplitude residuals. A time-lapse residual can be clearly interpreted by 2021 March 1 (Figure 1b). P-wave velocity reduction from the gaseous CO₂ plume decreased the impedance contrast at the top and bottom of the BBRs reservoir, causing a trough-peak time-lapse amplitude residual with side-lobe energy. The 2021 March 1st residual was originally interpreted as being caused by a gas-phase CO₂ plume within the perforated BBRs interval, expanding asymmetrically around the injection well (Kolkman-Quinn, 2022a,b). A follow-up survey on 2021 March 25 confirmed the 2021 March 1 result with a similar time-lapse image (Figure 1c). With continued injection and plume growth, subsequent VSP monitoring was expected to show both lateral expansion of the time-lapse anomaly and greater residual amplitude caused by further BBRs acoustic impedance reduction from increasing CO₂ saturation. However, later 2021 and 2022 monitor surveys also detected vertical expansion of the CO₂ residual (Figure 1 d-f). The appearance of an earlier time-lapse anomaly, overlapping and interfering with the BBRs anomaly, indicated the presence of partial gas saturation above the perforated BBRs interval, accumulating in a shallower interval within the water-saturated storage complex.

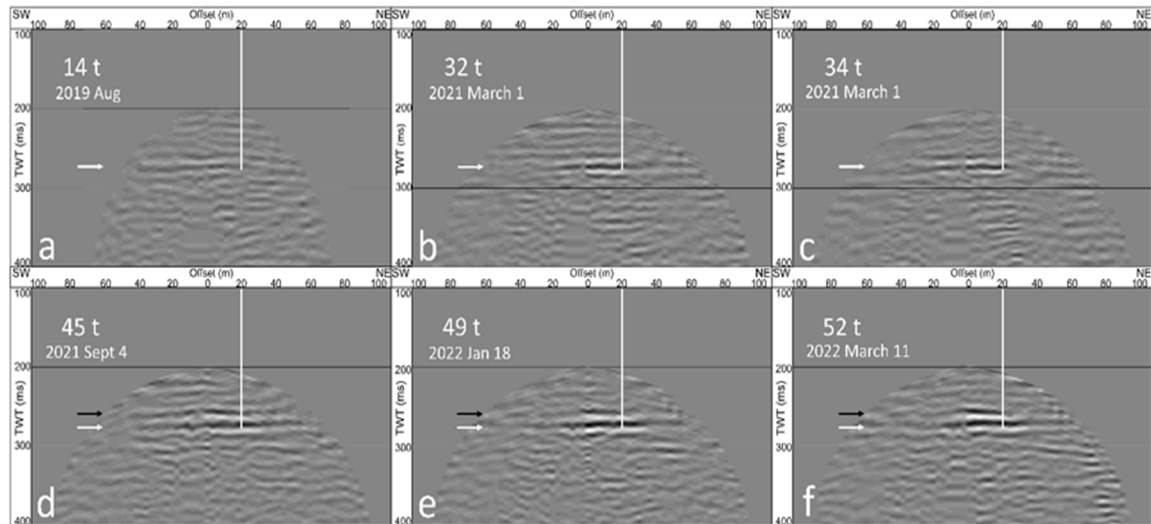


FIG. 1. VSP CDP time-lapse sections showing the difference between baseline 2017 May data and monitor data acquired on (a) 2019 August 27 (b) 2021 March 1, (c) 2021 March 25, (d) 2021 September 4, (d) 2022 January 18, and (f) 2022 March 11. The injection well's projected location is indicated by a vertical white line. The white arrow indicates the BBRs interval, and the black arrow indicates a time-lapse anomaly from a shallower interval.

Figure 2 shows the 2nd order difference between the 2021 March 1 and 2022 March 11 monitoring surveys, obtained by subtracting the b & c panels in Figure 1. In the perforated BBRS interval and above, CO₂ saturation increased sufficiently over 12 months to cause reflection amplitude changes in one or more layers above the perforated Basal Belly River Sandstone.

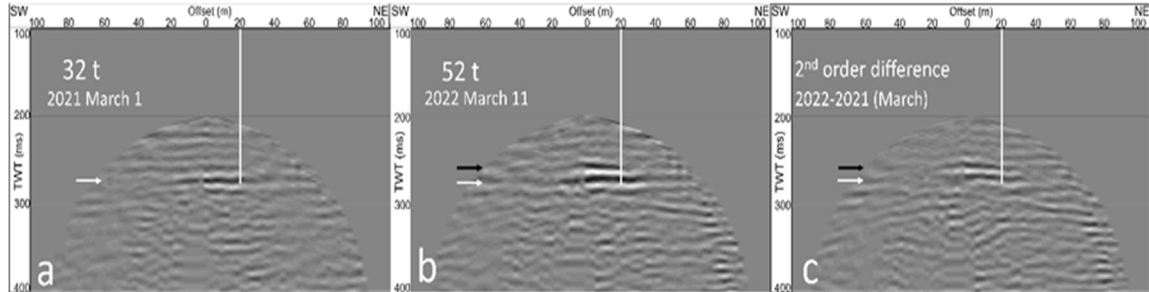


FIG. 2. Subtracting the 2022 March 11 – 2017 May (a) and the 2022 March 1 – 2017 May (b) time-lapse images from Figure 1 yielded a 2nd order difference (c) showing residual reflection amplitudes at both the BBRS and a shallower interval.

Timelapse ERT data

An array of permanent electrodes is installed at the Newell County Facility, as illustrated in Figure n. There are 16 cemented on the outside of the fibreglass casing in Obs 2 (Figure 3). In this well, the electrodes are spaced every 5 m between depths of 250 and 325 m KB. As shown in Figure 3, these electrodes straddle the BBRS from depths of 295 to 302 m KB. Along the ground surface, 112 electrodes at spacing of 10 m are buried 1.3 m deep in a 1.1 long km trench that also hosts fibre optic cables (Lawton et al., 2017).

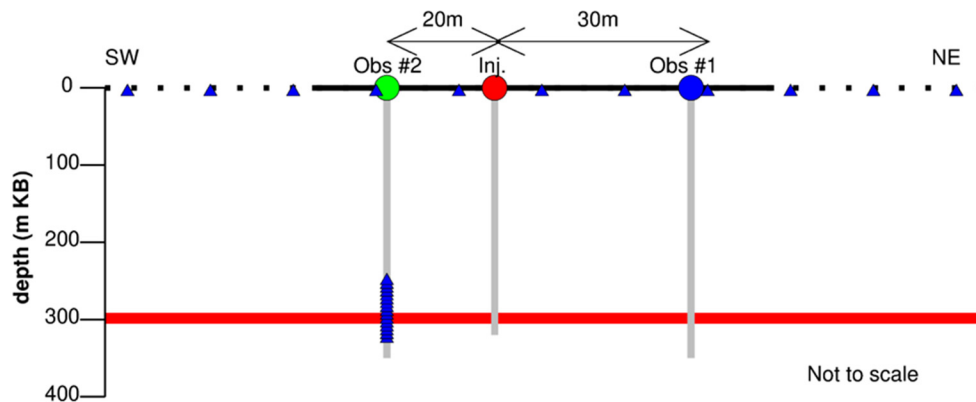


FIG. 3. Schematic diagram of the ERT installation. The red layer (295 to 302 m KB deep) is the BBRS injection zone. The trench hosts 112 electrodes (10 m spacing); Observation well #2 hosts 16 electrodes (from 250 to 325 m KB, at a spacing of 5 m, cemented outside the well casing).

The ERT measurement system is from Multi-Phase and consists of one data acquisition system (DAS) and a multiplexer, each hosting 64 electrodes. The objectives of the surveys are to collect time-domain resistivity data, with initial results presented by Macquet et al. (2021) and updated in this report. Borehole surveys are undertaken daily from September 2019 to May 14, 2021 and in this paper, we focus on results from 276 dipole-dipole configurations (normal and reciprocal) acquired from September 2019 to May 2022 with

the 16 borehole electrodes; the borehole surveys are more sensitive to CO₂ saturation in the BBRs than the surface electrodes due to the small volume of CO₂ injected to date. For the surveys, a maximum dipole separation of 25 m and a maximum dipole length of 25 m were used.

Figure 4 shows the evolution of the resistivity ratio (R/R_0) of the raw data, using the average of survey results recorded over the last 10 days of September 2019 to represent the baseline resistivity. Since CO₂ has a higher resistivity compared to the native brine, an increase of the resistivity ratio can be attributed to the brine being replaced by CO₂ injected into the pore spaces. Since only one observation well is equipped with electrodes, we assume the observed resistivity to be radially symmetric around the well but we represent the time series as a function of the distance between the observation and injection wells. It may lead to underestimated value of the resistivity change if the observed measurements are in fact the average of saturated and unsaturated areas around and proximal to the observation well as the CO₂ plume approaches it and replaces the brine.

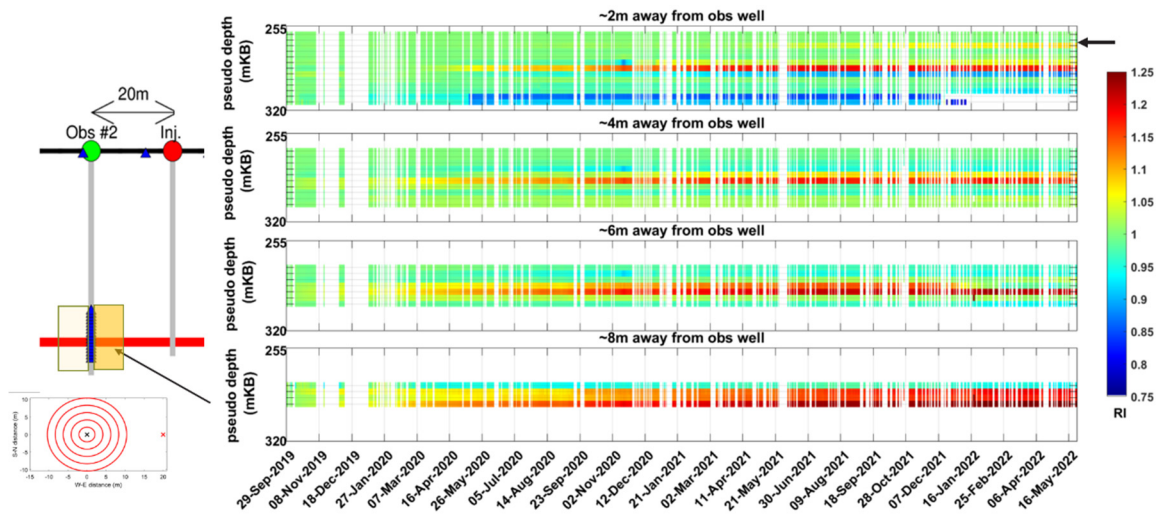


FIG. 4. Resistivity ratio of the raw data for dipole-dipole configurations in Obs2. Pseudo-distances away from the observation well are computed using the locations of the electrodes. We use the average of the 10 last days of September 2019 for the baseline measurements,

From Figure 4 we see that the resistivity ratio increases earlier in time with increasing pseudo-distance away from the observation well, meaning that the CO₂ is initially close to the injection well, as expected. The presence of CO₂ as early as October 2019 is interpreted at a pseudo-distance of 8 m from the observation well, whereas the presence of CO₂ at a pseudo-distance of 2 m from the observation well is not observed until March 2020. However, by May 2022, a resistivity ratio anomaly is observed at all pseudo-distances, but the highest ratio at the pseudo-distance of 8 m, which we interpret to indicate a higher CO₂ saturation level closer to the injection well. Also important is a thin resistivity ratio anomaly at the 2 m pseudo-distance but at a shallower depth (arrowed) than the main anomalies. This anomaly first appears in April 2021 and slowly increases through to May 2022. Figure 5 show a graph of the main resistivity ratio anomalies in the injection zone

(lower graph) for all pseudo-distances, as well the ratio for the shallower layer (upper graph). It is noteworthy that the increase in the resistivity ratio in the shallower layer coincides with the relatively constant resistivity ratios in the main injection zone,

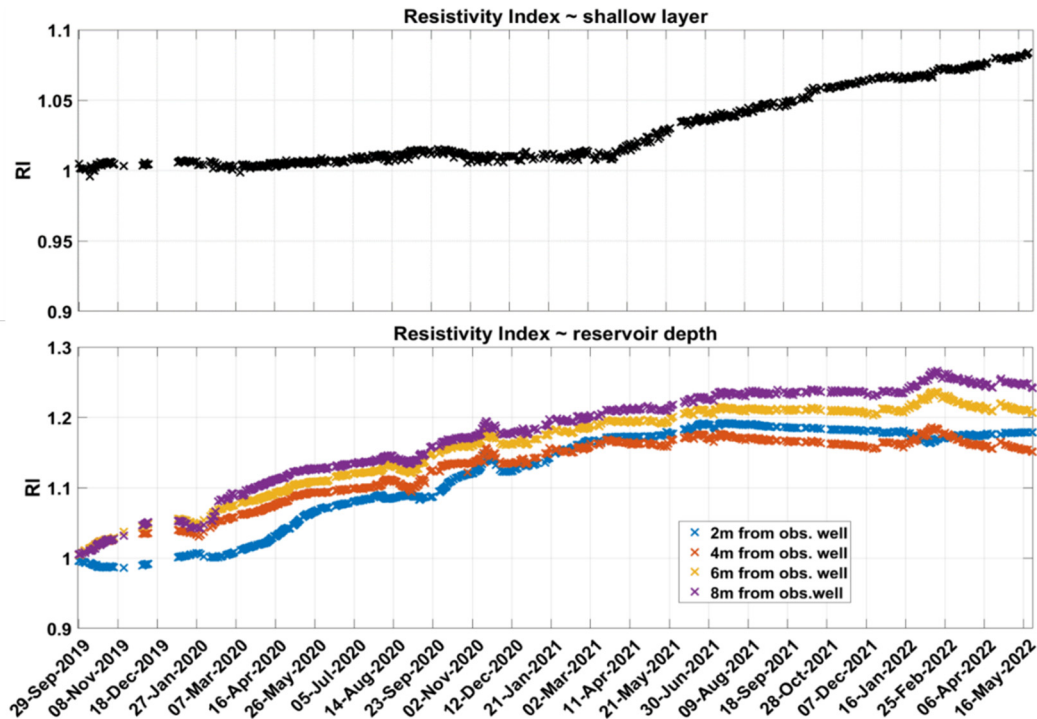


FIG. 5. Change in the resistivity ratio from September 2019 to May 2022 at a pseudo-distance of 2 m in the shallow layer (upper graph) and for all pseudo-distances in the main injection zone (lower graph). Note that the increasing resistivity ratio in the upper thin layer coincides with constant resistivity ratios in the injection zone.

Discussion

From both the timelapse VSP and ERT data, it is clear that upward migration of CO₂ in the storage complex has occurred, starting in about the spring of 2021 and continuing into the current year, as evidenced by the March 2022 VSP survey and the May 2022 ERT survey. Having two independent datasets showing these results provides compelling evidence supporting this interpretation.

MONITORING FOR GIGATONNE GCS

For monitoring large-scale GCS projects, the regulatory requirements in Alberta have the following principles for measurement, monitoring and verification (MMV) for secure storage (Govt of Alberta, 2022):

- Regulatory compliance
- Project and site specific; address regional impacts
- Risk-based and fit-for-purpose (e.g. induced seismicity, interference)
- Adaptive, with elaboration through successive project stages
- Provide timely warning of containment and conformance anomalies
- Monitorability in geosphere, hydrosphere, biosphere, and atmosphere.

- Transparency
- Best available technologies economically achievable (BATEA) - based on sound science and engineering

It can be challenging to meet all of these requirements, particularly to provide timely warning of containment or conformance anomalies yet be able to do this through the BATEA principle. One approach is to move to sparse monitoring using spatially separated monitoring nodes. As an example, Figure 6 shows the approximate diameters of a CO₂ plume in a key saline aquifer in Alberta – the Basal Cambrian Sand – after 10 Mt and 1 Gt of injection. For these simple analyses, we assume porosity of 10%, thickness of 50 m, temperature of 75°C, initial reservoir pressure of 25 MPa and a storage efficiency factor (SEF) of 7%. At this temperature and pressure, the density of CO₂ is 710 kg/m³.

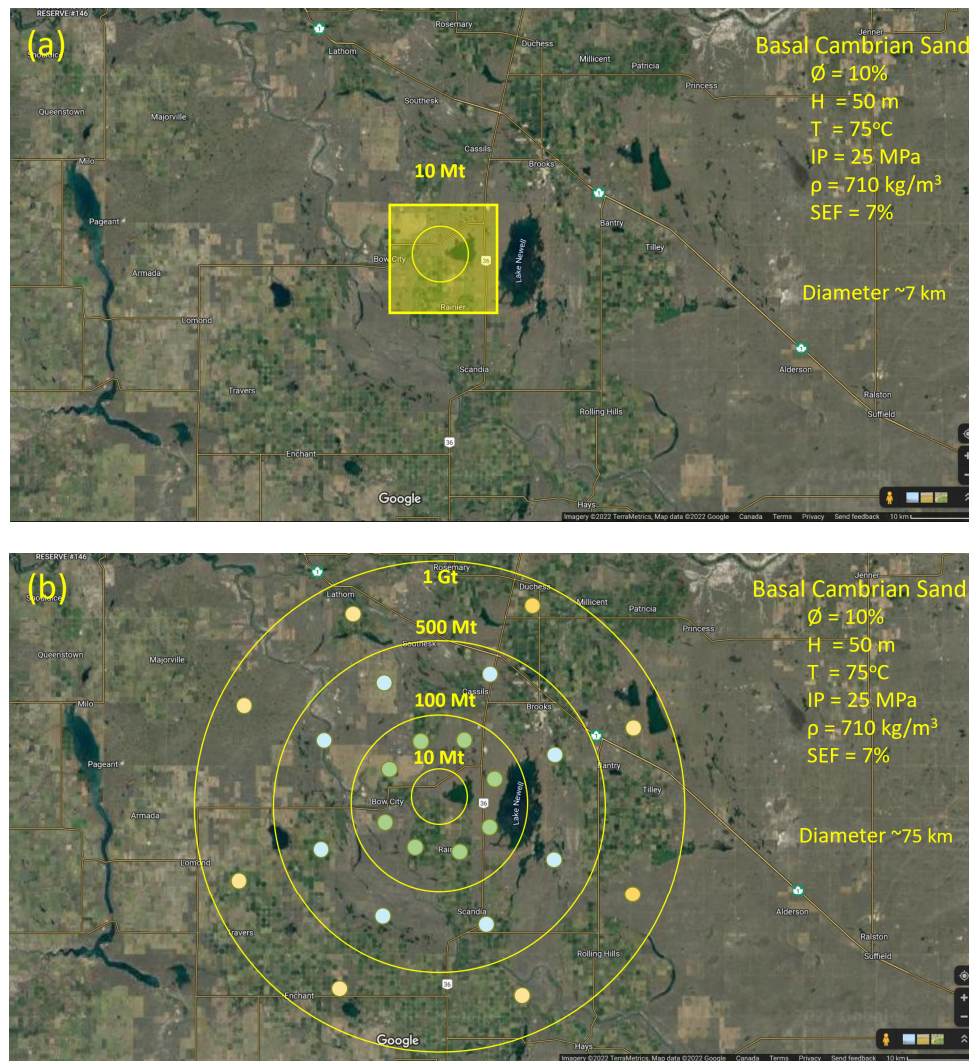


FIG. 6. (a) Diameter of plume after 10 Mt of CO₂ is ~ 7 km; (b) after 1 Gt of injection the diameter is ~75 km. A simple disk model into an homogeneous reservoir is assumed. Different monitoring approaches are illustrated with a standard 3D seismic survey (highlighted rectangle) for the 10 Mt scenario and using nodes for larger injection scenarios (coloured dots).

Initially, as seen from the CMC and other GCS projects, such as Quest, walkaway VSP surveys are optimum for imaging the CO₂ plume around the injection well. Also, VSP and ERT surveys are very useful if there are targeted areas of concern in the area of interest during later stages of a GCS program when the plume is much larger. After about 5-10 Mt of injection, VSP surveys centered on the injection well will not image the leading edge of the plume very well and seismic monitoring using 3D surface seismic surveys is more appropriate. However, at injection volumes of greater than 10-100 Mt, 3D seismic surveys become more difficult from both a cost and logistics perspective and here we propose sparse, nodal surveys, as shown schematically in Figure 6b.

For seismic monitoring of GCS projects there are 4 main challenges - repeatability, resolution, how often we repeat the seismic surveys, and the cost of full-scale surveys that extend over the anticipated area of the CO₂ plume and/or pressure front. One monitoring approach is to use sparse nodes of sub-permanent seismic sources and permanent receivers that can be deployed on an expanding basis during the injection program as the plume develops. Interest has been developing in permanent reservoir monitoring for GCS projects to not only track the plume but to capture transient changes that might occur in the reservoir. Surface orbital vibrators mounted on concrete foundations have been developed with good results shown from Otway (Australia) and EEERC in North Dakota (US) are examples of source nodes.

A challenge for surface sources and receivers used for time-lapse land seismic data is separating time delays caused by seasonal changes in the near surface from 4D effects related to CO₂ injection (Henley and Lawton, 2020). To overcome this, at the Newell County Facility we have been testing permanent sources (GPUSA orbital vibe and a 'Squid' 3P Technology impulsive plasma source) mounted on a large helical screw pile (pedestal) that are screwed into the ground into bedrock below the weathering layer (Spackman and Lawton, 2019) and recording into an array of geophones cemented into the geophysics observation well. This receiver array is composed of 24 x 3C geophones mounted on the outside of Obs2, from depths of 191 m to 306 m.

Figure 7 shows a comparison of VSP reflection data gather from the plasma source compared to an equivalent gather using a surface Envirovibe source. The Squid data are clearly earlier in time compared with the Envirovibe data, indicating that the source energy is coupling to the ground directly into the bedrock at the base of the pedestal. The Squid data also has broader bandwidth than the Envirovibe data, as shown by the amplitude spectra below each gather.

The concept of single source and a single or a small number of receivers has been implemented previously (e.g. Brun et al. 2021). In this report we propose an advancement by designing the survey using an optimum offset approach (Hunter and Pullan, 1989) where the source – receiver offset is selected so that the reflection is captured at an offset that is beyond the arrival times of surface waves and inside the first arrival times and associated reverberations, in order to maximize S/N.

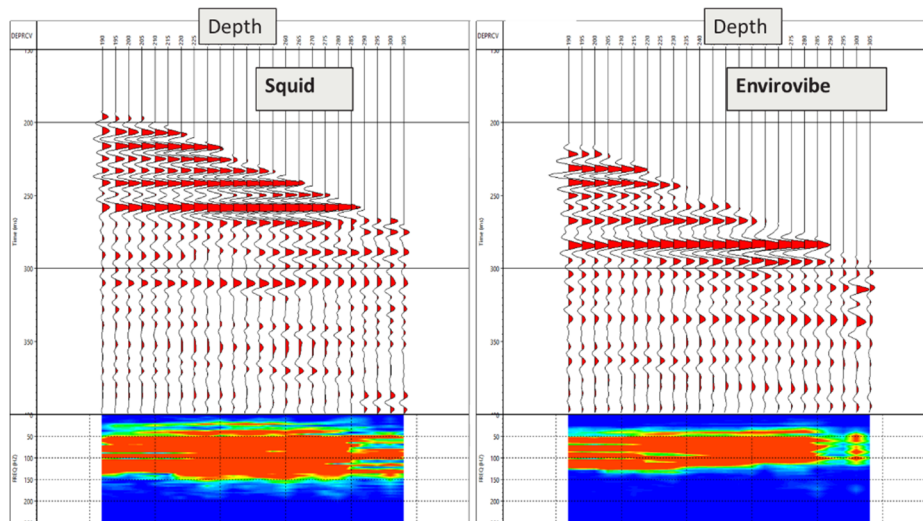


FIG. 7. Prestack gathers of the upgoing reflection data from Squid (left) and Envirovibe (right) sources.

Figure 8 shows a typical full-offset shot gather recorded in southern Alberta, to illustrate the optimum offset concept. The yellow highlighted areas identifies the ‘optimum offset window’ in which reflections have the highest S/N. The red lines outline reflectors that could be CO₂ injection zones.

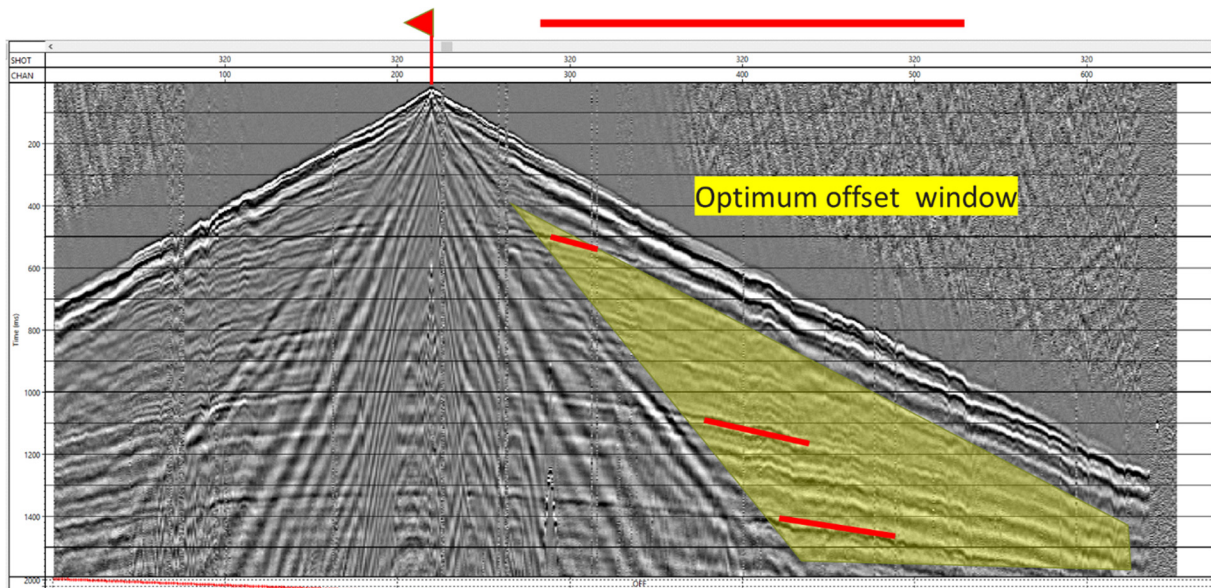


FIG. 8. Shot gather showing optimum offset window for designing sparse nodes, in which reflection S/N is highest.

The advantage of this approach is that the reflection from the CO₂ reservoir is a clean event that is not corrupted by non-stationary source-related noise. Thus small changes in reflection amplitude and travel time can be recorded and analyzed in a 4D sense to interpret the arrival of the CO₂ plume at this survey location.

The advantage of using the source pedestal approach is due to not only to avoid changes due to seasonal variations in the near-surface, but also that the seismic source can be moved easily from one pedestal location to another; i.e. multiple source equipment is not required.

The sparse node concept can also be expanded to incorporate many other measurements in addition to seismic surveys for monitoring GCS projects at large scale. Figure 9 shows a schematic diagram of how a node may be designed. In addition to the permanent seismic source and receivers, one or more shallow wells could also be drilled and equipped with optical fibre and technologies to enable VSP, ERT, EM, gravity and tilt surveys to be undertaken, as well as sampling of groundwaters and deeper aquifers. The permanent geophone array can also be used for microseismic monitoring when active source seismic acquisition is not being undertaken.

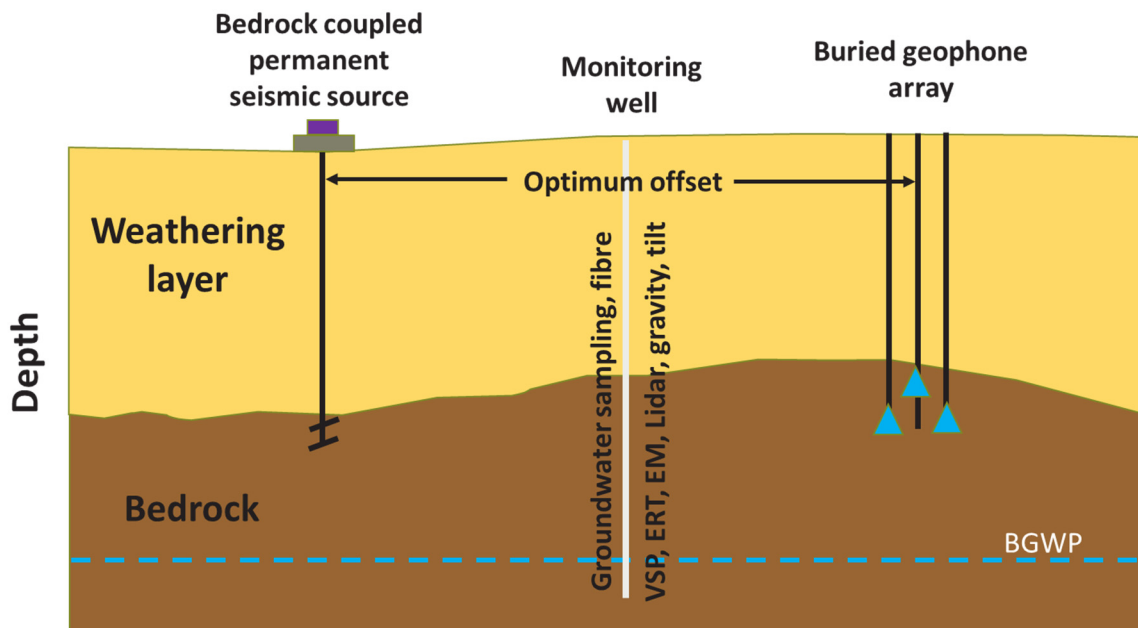


FIG. 9. Schematic of a node layout including a permanent seismic source and receivers, as well as a monitoring well for other monitoring datasets. An array of such nodes could be deployed for large-scale geological carbon storage projects.

Conclusions

Timelapse VSP and ERT surveys at the Newell County Facility have been successful in establishing a CO₂ detection threshold of ~34 tonnes at the injection depth of 300 m at the site. These results demonstrate that that these technologies can be used as early warning methodologies to detect upward migration of CO₂ from a deep GCS project if a leakage is suspected.

We also introduce a refined approach to permanent source – minimal receiver effort seismic surveys for monitoring GCS projects at large scale. The advantage of using the source pedestal approach is not only to avoid changes due to seasonal variations in the near-surface rocks, but also that the seismic source can be moved easily from one pedestal

location to another; i.e. multiple sources are not required. This approach could also be integrated with passive seismic and other monitoring techniques at each survey location through the development of comprehensive nodes.

Acknowledgements

We thank CaMI.FRS JIP members, CREWES sponsors and 3P Technologies Inc for their support for this project. The authors also acknowledge financial support from the University of Calgary's Canada First Research Excellence Fund program: The Global Research Initiative in Sustainable Low-Carbon Unconventional Resources. We also thank Schlumberger for Vista software licenses for processing the VSP data collected at the site.

REFERENCES

- Victoria Brun, Elodie Morgan, Brad Gerl, Luis Cardozo, Richard Habiak, 2021, Light time-lapse seismic monitoring for SAGD: a new approach & operational model. GeoConvention, Calgary. <https://spotlight-earth.com/geoconvention-2021-paper-5>
- David C. Henley and Donald C. Lawton, 2021, Time-lapse detection using raypath interferometry, *GEOPHYSICS* 86: Q27-Q36. <https://doi.org/10.1190/geo2020-0562.1>
- Hunter, J.A., and Pullan, S.E, 1989, The shallow seismic optimum offset shallow technique. SEG Annual General Meeting.
- Kolkman-Quinn, B., 2022a, Time-lapse VSP monitoring of CO₂ sequestration at the CaMI Field Research Station: M.Sc. Thesis, University of Calgary.
- Kolkman-Quinn, B., Lawton, D., Macquet, M., *under revision*, CO₂ leak detection threshold using vertical seismic profiles, *International Journal of Greenhouse Gas Controls*.
- Kolkman-Quinn, B., Lawton, D., 2022b., Detection threshold of a shallow CO₂ plume with VSP data from the CaMI Field Research Station. IMAGE 2022, Houston, TX, USA.
- Lawton, D., Dongas, J., Osadetz, K., Saeedfar, A., & Macquet, M., 2019, Development and Analysis of a Geostatic Model for Shallow CO₂ Injection at the Field Research Station, Southern Alberta, Canada. In T. Davis, M. Landrø, & M. Wilson (Eds.), *Geophysics and Geosequestration* (pp. 280-296). Cambridge: Cambridge University Press. doi:10.1017/9781316480724.017.
- Macquet, M., Lawton, D.C., Saeedfar, A. and Osadetz, K.G., 2019, A feasibility study for detection thresholds of CO₂ at shallow depths at the CaMI Field Research Station, Newell County, Alberta, Canada. *Petroleum Geoscience*, 25(4), pp.509-518.
- Macquet, M., Lawton, D. C., Rippe, D., & Schmidt-Hattenberger, C., 2021, September, Semi-continuous electrical resistivity tomography monitoring for CO₂ injection at the CaMI Field Research Station, Newell County, Alberta, Canada. In *First International Meeting for Applied Geoscience & Energy* (pp. 362-366). Society of Exploration Geophysicists.
- Macquet M., Lawton G., Osadetz K., Maidment G., Bertram M., Kolkman-Quinn B., Monsegny Parra J., Raad S. M. J. , Race F., Savard G., Yang Y., 2022, Overview of Carbon Management Canada's pilot-scale CO₂ injection site for developing and testing monitoring technologies for carbon capture and storage, and methane detection, *Recorder*, Focus Article, 27 p., <https://csegrecorder.com/articles/>

Tyler W. Spackman, Donald C. Lawton and Malcolm B. Bertram, 2019, Seismic data acquired with a novel, permanently-installed borehole seismic source. SEG Annual General Meeting. <https://doi.org/10.1190/segam2019-3214836.1>